Immunity, Vol. 22, 105–115, January, 2005, Copyright ©2005 by Elsevier Inc. DOI 10.1016/j.immuni.2004.12.006

Absence of the Endothelial Oxidase AOC3 Leads to Abnormal Leukocyte Traffic In Vivo

Craig M. Stolen,[1,3] Fumiko Marttila-Ichihara,[1,3] Kaisa Koskinen,[1] Gennady G. Yegutkin,[1] Raisa Turja,[1] Petri Bono,[1,4] Mikael Skurnik,[2] Arno Hänninen,[1] Sirpa Jalkanen,[1] and Marko Salmi[1,*]

[1]Department of Medical Microbiology
MediCity Research Laboratory
National Public Health Institute
Turku University
20520 Turku
Finland

[2]Department of Bacteriology and Immunology
Helsinki University
University of Helsinki
00290 Helsinki
Finland

Summary

Leukocyte migration from the blood to tissues is a prerequisite for normal immune responses. We produced mice deficient in an endothelial cell-surface oxidase (amine oxidase, copper containing-3 [AOC3], also known as vascular adhesion protein-1 [VAP-1]) and found that this enzyme is needed for leukocyte extravasation in vivo. Real-time imaging shows that AOC3 mediates slow rolling, firm adhesion, and transmigration of leukocytes in vessels at inflammatory sites and lymphoid tissues. Absence of AOC3 results in reduced lymphocyte homing into lymphoid organs and in attenuated inflammatory response in peritonitis. These data alter the paradigm of leukocyte extravasation cascade by providing the first physiological proof for the concept that endothelial cell surface enzymes regulate the development of inflammatory reactions in vivo and suggest that this enzyme should be useful as an anti-inflammatory target.

Introduction

Leukocyte traffic between the blood and tissues is needed for normal immune homeostasis as well as for mounting adequate inflammatory responses. The spectrum of inflammatory diseases for which the inadvertent migration of leukocytes is proving to be critical is increasing all the time. Therefore, understanding of the mechanisms of how leukocytes leave the blood and enter tissues is critical for understanding the pathogenesis of inflammatory reaction and for the development of novel anti-inflammatory strategies (Nathan, 2002).

Different steps of the leukocyte extravasation cascade—tethering, rolling, activation, firm adhesion, and transmigration—can be mediated by traditional adhesion and activation molecules (von Andrian and Mackay, 2000). Selectins and their sialomucin ligands contribute to the initial shear-dependent interactions between the vascular endothelium and blood-borne leukocytes (Ley and Kansas, 2004; Rosen, 2004). If rolling cells receive appropriate activating signals from chemokines, they can firmly bind to the endothelial cells (Kunkel and Butcher, 2002; Miyasaka and Tanaka, 2004). The firm adhesion and the subsequent transmigration step are mediated by leukocyte integrins and adhesion molecules belonging to the immunoglobulin superfamily (Dejana, 2004; Muller, 2003; Pribila et al., 2004). However, the tissue selectivity and kinetics of leukocyte extravasation in such a complex process can only be partly explained by the function of these well-established molecules.

We have previously provided in vitro evidence that antibodies against AOC3 (also known as EC1.4.3.6, placental amine oxidase, or VAP-1) partially block leukocyte-endothelial interactions (Koskinen et al., 2004; Lalor et al., 2002; Salmi and Jalkanen, 1992; Salmi et al., 1997, 2001; Smith et al., 1998), suggesting that AOC3 may be involved in leukocyte binding to vessels. This enzyme belongs to semicarbazide-sensitive amine oxidases (SSAO), which catalyze oxidative deamination of primary amines in a reaction producing bioactive aldehydes, hydrogen peroxide, and ammonium as end products (Jalkanen and Salmi, 2001; Klinman and Mu, 1994). The enzymatic properties of SSAO have been known for decades, but their physiological functions have remained elusive.

To study the physiological functions of AOC3 in vivo, we produced AOC3-deficient mice and analyzed leukocyte traffic in them. Real-time imaging and various disease models showed that AOC3 is needed for normal leukocyte extravasation both under normal conditions and in inflammation. The results are direct physiological proof that a cell-surface enzyme is critical for the leukocyte migration in vivo.

Results

AOC3-Deficient Animals Lack All SSAO Activity

To understand the physiological functions of SSAO/AOC3, gene targeting techniques were used to disrupt the mouse *AOC3* gene by replacing a portion of its first exon with a neomycin-resistance (Neo^r) cassette (Figure 1A). Mice homozygous for the null mutation on a pure 129 background were produced. Gene disruption and zygosity were verified by Southern blots (Figure 1B) and/or PCR (Figure 1C).

The absence of AOC3 expression in homozygous null mutant mice was confirmed at the transcriptional level by RT-PCR by using total RNA from mouse small intestine, heart, and liver (data not shown). Furthermore, no AOC3 protein expression was found in any tested organ of *AOC3*$^{-/-}$ mice by immunostainings with three different anti-mouse AOC3 monoclonal antibodies (mAb) (Figure 1D and data not shown). In wild-type (wt) control mice AOC3 protein expression was found in the endo-

*Correspondence: marko.salmi@utu.fi
[3]These authors contributed equally to this work.
[4]Present address: Department of Oncology, Helsinki Central University Hospital, Helsinki, Finland.

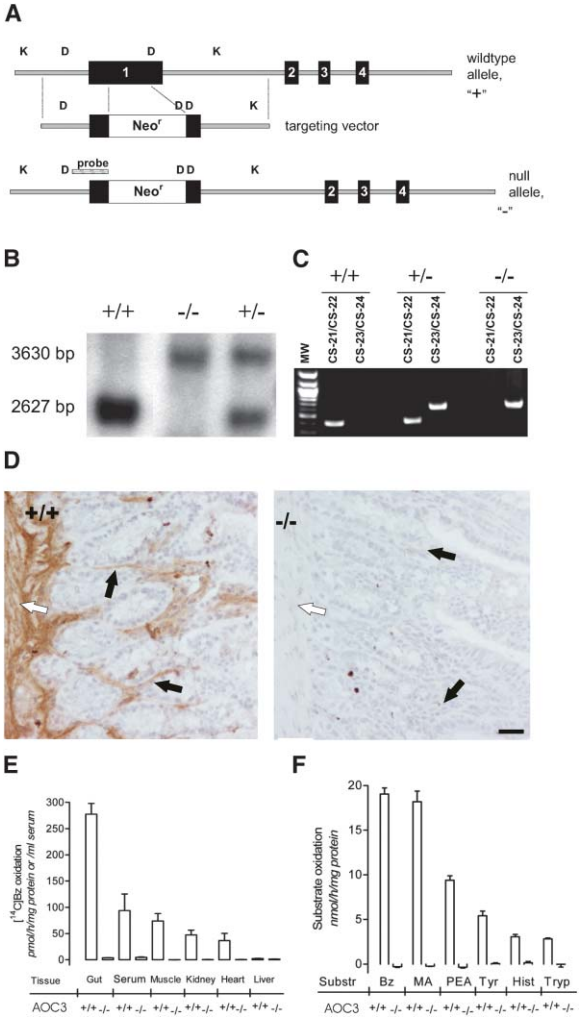

Figure 1. Disruption of the *AOC3* Gene in Mice Leads to an Absence of SSAO Activity

(A) The structure of the *AOC3* gene with four exons, the targeting construct and the null allele are shown diagrammatically. Digestion sites for DraIII (D), KpnI (K), and the probe used in Southern blotting are indicated.

(B) Southern blot analyses of DNA isolated from wild-type (+/+), heterozygous (+/−), and *AOC3* knockout (−/−) animals digested with *Dra*III and probed with the probe A is shown. The wild-type (wt) allele yields a band at 2627 bp and the targeted allele at 3630.

(C) PCR analyses of mouse genotypes. Genomic DNA was amplified with the indicated primer pairs specific for Neo^r (CS23 and CS24, a 604 bp product) and for wt allele of *AOC3* (CS21 and CS22, a 405 bp product) and analyzed in agarose gels.

(D) AOC3 protein is absent from *AOC3*$^{-/-}$ animals. Small intestine sections were stained immunohistochemically with anti-mouse AOC3-specific mAb. AOC3 (brown precipitate) is present in the endothelial (some pointed out by black arrows) and smooth muscle (white arrow) cells in the wt animals but completely absent in *AOC3*$^{-/-}$ animals. Bar, 50 μm.

(E) No detectable SSAO activity in *AOC3*$^{-/-}$ animals. SSAO activity was assayed radiochemically in the serum and tissue lysates of wt and AOC3-deficient animals. Error bars are ± SEM.

(F) SSAO activity was also tested fluorimetrically in adipose lysates by using benzylamine (Bz); methylamine (MA), phenylethylamine (PEA), tyramine (Tyr), histamine (Hist), and tryptamine (Trp) as substrates in the *AOC3*$^{-/-}$ and wt animals. Error bars are ± SEM.

thelium, smooth muscle, and adipose tissue, as expected.

The gene targeting of mouse AOC3 resulted in a complete ablation of all detectable SSAO activity from various tissues and serum in enzyme assays (Figure 1E). None of the six potential substrates (benzylamine, methylamine, phenylethylamine, tyramine, tryptamine, or histamine) were oxidized in an SSAO-dependent manner in *AOC3*$^{-/-}$ animals, whereas detectable activity was present in the wt littermates (Figure 1F).

Together these data show that there is no AOC3 mRNA, protein, or SSAO activity in *AOC3*$^{-/-}$ mice. Our data suggest that the *AOC3* gene is the major source of mouse SSAO, although there are at least two other SSAO genes in these animals as in humans (Chassande et al., 1994; Imamura et al., 1998).

AOC3-Deficient Animals Develop Normally

In a specific pathogen-free environment, the adult *AOC3*$^{-/-}$ mice in 129S6 background showed no overt phenotype, were healthy by visual inspection, maintained a normal body weight, and had a full life span (some original *AOC3*$^{-/-}$ mice were maintained for over 2 years). There were no overt macroscopic or microscopic changes in any tissues or organs analyzed in AOC3-deficient animals. Both sexes were fertile, and the AOC3-mutated allele was found in the offspring in the expected Mendelian ratio.

To elucidate the potential role of AOC3 in immune defense, we analyzed the leukocytes and vasculature in more detail. We found no statistically significant differences between *AOC3*$^{-/-}$ animals and wt controls in the absolute numbers of leukocytes in blood or in peripheral lymph nodes, Peyer's patches, mesenteric lymph nodes, or spleen, although AOC3-deficient animals had somewhat fewer lymphocytes in all these lymphoid organs (Tables 1 and 2). The proportions of leukocyte subclasses in blood and those of CD4- and CD8-positive T cells and B cells in the thymus and secondary lymphoid organs were similar in the wt and AOC3-deficient animals (Tables 1 and 2 and data not shown; $p > 0.05$ for all comparisons). On the vascular side, the endothelium was morphologically intact in AOC3-deficient animals in the inflamed vascular bed of cremaster muscles (Figure 2A and 2B) and in high endothelial venules in Peyer's patches (Figure 3A and 3B). The hemodynamic parameters were also similar between the two groups (Table 1; $p > 0.05$ for all comparisons). Thus, AOC3 alone is not needed for normal development, and its absence does not cause any obvious impairment of immune surveillance under specific pathogen-free conditions.

Extravasation of PMN Is Impaired in Inflammation in *AOC3*$^{-/-}$ Animals

To study the potential physiological functions of AOC3 in immune defense, we first analyzed leukocyte extravasation cascade in *AOC3*$^{-/-}$ animals. Intravital videomicroscopy of inflamed cremaster muscle (500 ng TNF-α intrascrotally for 3 hr) allows direct examination of the interactions between polymorphonuclear leukocytes (PMN), which comprise >90% of interacting cells in this model and the blood vessel wall (Ley et al., 1995). The rolling velocity of PMN was about five times faster in

Table 1. Hematological and Hemodynamic Characteristics of *AOC3*$^{-/-}$ Mice

Parameter	Wt	*AOC3*$^{-/-}$
Blood cell counts (n = 10/group)		
Total leukocytes ($\times 10^9$/L)	3.0 ± 0.5[a]	3.7 ± 0.3[b]
Lymphocytes	69.5% ± 2.4%	71.4% ± 1.2%
Neutrophils	23.4% ± 2.2%	22.1% ± 1.3%
Eosinophils	1.1% ± 0.1%	1.0% ± 0.1%
Basophils	1.3% ± 0.1%	1.3% ± 0.1%
Monocytes	4.7% ± 0.4%	4.2% ± 0.4%
Erythrocytes ($\times 10^{12}$/L)	7.0 ± 0.5	6.6 ± 0.5
Platelets ($\times 10^9$/L)	30.7 ± 4.6	34.0 ± 2.7
Hemoglobin (g/L)	12.8 ± 0.6	12.3 ± 0.6
Vessels		
Cremaster: mild inflammation		
Animals (n)	5	5
Vessels (n)	167	110
Diameter (μm)	22.0 ± 1.2	23.2 ± 0.7
Wall shear rate (s^{-1})	1092 ± 134	965 ± 239
Cremaster: strong inflammation		
Animals (n)	5	5
Vessels (n)	170	161
Diameter (μm)	27.7 ± 0.4	27.5 ± 1.0
Wall shear rate (s^{-1})	533 ± 10	562 ± 231
Peyer's patch HEV		
Animals (n)	5	5
Vessels (n)	131	99
Diameter (μm)	15.6 ± 1.1	15.8 ± 2.0
Wall shear rate (s^{-1})	820 ± 109	871 ± 141
Cremaster: anti-AOC3 mAb		
Animals (n)	5	5
Vessels (n)	13	31
Diameter (μm)	43.1 ± 4.8	46.5 ± 2.3
Wall shear rate (s^{-1})	874 ± 136	906 ± 141
Cremaster: anti-L-selectin mAb		
Animals (n)	4	4
Vessels (n)	30	24
Diameter (μm)	44.8 ± 2.1	45.2 ± 5.2
Wall shear rate (s^{-1})	1064 ± 202	1091 ± 125

[a] Mean ± SEM.
[b] The difference in any of the variables measured is not statistically significant between the two genotypes.

animals lacking AOC3 (Figure 2C and Movies S1 and S2 available online at http://www.immunity.com/cgi/content/full/22/1/105/DC1), although the number of PMN that rolled on the endothelium (rolling flux; Figure 2D) was not altered. In AOC3-deficient animals there was also almost a 50% reduction in the number of stably bound PMN when compared to the controls (Figure 2E). When the number of firmly adherent leukocytes was normalized to the rolling leukocyte pool available for interactions in the same vessel, we noted that the efficiency of the firm adhesion step was 3.2 times higher in the wt than in the *AOC3*$^{-/-}$ animals. We also observed that there were fewer PMN that had transmigrated out from the vessel in AOC3-deficient animals (Figure 2F), but the low numbers of extravasated cells even in the wt animals did not allow detailed analyses of the transmigration step in this model of relatively mild inflammation. These data thus show that AOC3 mediates at least slow rolling and firm adhesion of PMN in an inflamed vascular bed in vivo.

We next elicited a stronger inflammation in the cremaster (1.5 μg TNF-α intrascrotally for 6 hr) to dissect the contribution of AOC3 to the transmigration step in more detail. In this model, we also observed significantly increased rolling velocity, decreased firm adhesion, and decreased adhesion efficiency in *AOC3*$^{-/-}$animals (Figures 2G–2I). Increased numbers of transmigrated PMN were found in wt animals when compared to the milder inflammatory stimulus. Most notably, we found a 71% reduction in the number of transmigrated PMN outside the vessel wall at the scene of inflammation in *AOC3* knockout animals when compared to the wt controls (Figures 2J and 2K). To obtain a parameter describing the efficacy of this final step of the extravasation cascade, independent of the changes in the previous steps, we normalized the number of transmigrated cells to that of intravascular cells ready to transmigrate (i.e., firmly adherent cells). The analyses showed that the transmigration efficiency was reduced by 47% in the AOC3-deficient animals ($p = 0.01$).

We then studied the effect of a function-blocking anti-mouse AOC3 mAb in the same intravital model (Figures 4A–4C). The analyses of larger vessels in this series of experiments showed that in AOC3-deficient animals the leukocytes rolled faster ($p = 0.02$) and the cells had a tendency to adhere less efficiently ($p = 0.08$) than in the wt controls. When the anti-AOC3 mAb was injected intravenously into wt recipients that had been stimulated with TNF-α intrascrotally, we saw significantly increased rolling velocity of leukocytes (Figure 4A) and no significant change in the rolling flux (Figure 4B). The anti-AOC3 mAb had no significant effect on the number of firmly adherent cells (Figure 4C), which is in line with the fact that most adherent cells probably have adhered during the 6 hr induction of the inflammation when the mAb was not present. The antibody treatment also did not affect blood leukocyte counts (before injection, 9.0 ± 0.8; 15 min after the injection, 11.5 ± 0.5; and 30 min after the injection, 11.3 ± 0.8 × 10^6/ml [mean ± SEM, n = 3]) or wall shear rate (before and 30 min after the injection, 874 ± 136 and 863 ± 163 s^{-1} in the wt and 906 ± 141 and 898 ± 143 s^{-1} in the *AOC3*$^{-/-}$ mice, respectively). The same anti-AOC3 mAb showed no significant effects on the velocity or number of rolling or adherent leukocytes when it was administered into *AOC3*-deficient animals (Figures 4A–4C). These data confirm that the biological effects of this anti-AOC3 mAb are due to specific ligation of AOC3 in vivo.

The real-time imaging of leukocyte-endothelial cell contacts thus reveals that AOC3 is needed for PMN extravasation in an inflammatory lesion under physiological flow conditions in vivo. Intriguingly, in the multistep adhesion cascade, AOC3 appears to independently contribute to each of the three overlapping adhesive steps by mediating slow rolling, firm adhesion, and transmigration. Most importantly, in the absence of AOC3, the overall efficiency of inflammatory process (the number of transmigrated PMN per 1000 circulating leukocytes) was only 23% of that seen in the wt controls.

AOC3 Contributes to Constitutive Lymphocyte Homing

Lymphocytes continuously recirculate between the blood and lymphatic organs like Peyer's patches under normal conditions (von Andrian and Mempel, 2003). By

Table 2. Numbers of Leukocytes in Lymphoid Tissues of Wild-Type and AOC3$^{-/-}$ Mice

Wild Type[a]			AOC$^{-/-}$	
Tissue	Number of Leukocytes ($\times 10^6$)	Percentage of Total	Number of Leukocytes ($\times 10^6$)	Percentage of Total
PLN[b]	6.4 ± 0.8		4.6 ± 0.8	
CD4	4.0 ± 0.2	62.9% ± 3.0%	2.9 ± 0.0	63.7% ± 0.9%
CD8	1.3 ± 0.1	21.2% ± 0.9%	1.0 ± 0.0	21.0% ± 0.4%
B220	0.7 ± 0.1	11.1% ± 1.6%	0.5 ± 0.0	10.6% ± 0.9%
MLN	19.3 ± 2.3		15.2 ± 1.5	
CD4	9.1 ± 0.6	47.1% ± 3.0%	8.4 ± 0.2	55.2% ± 1.6%
CD8	4.3 ± 0.6	22.2% ± 3.0%	3.0 ± 0.2	20.0% ± 1.5%
B220	5.0 ± 0.5	25.7% ± 2.4%	3.5 ± 0.4	23.2% ± 2.6%
PP[c]	5.6 ± 0.7		3.7 ± 1.2	
CD4	2.0 ± 0.1	35.9% ± 2.0%	1.2 ± 0.1	31.9% ± 1.8%
CD8	0.3 ± 0.0	5.6% ± 0.6%	0.2 ± 0.0	5.1% ± 0.5%
B220	2.9 ± 0.2	51.4% ± 3.8%	1.9 ± 0.2	50.4% ± 5.2%
Spleen	57.0 ± 4.4		48.6 ± 0.3	
CD4	15.1 ± 1.0	26.4% ± 1.8%	13.4 ± 1.5	27.5% ± 3.0%
CD8	6.2 ± 1.3	10.9% ± 2.3%	6.0 ± 1.2	12.3% ± 2.4%
B220	23.7 ± 1.9	41.7% ± 3.3%	21.1 ± 1.4	43.5% ± 2.8%

[a] Data (mean ± SEM) are from 12 wt and 8 AOC3-deficient animals.
[b] PLN, peripheral lymph nodes (inguinal and axillar lymph nodes); MLN, mesenteric lymph node; and PP, Peyer's patch.
[c] Total number of lymphocytes in all identified Peyer's patches. There were no differences in the number of Peyer's patches between the two genotypes.

using intravital videomicroscopy and fluorescently labeled cells, we observed that the lack of AOC3 caused remarkable increase of rolling velocity when lymphocytes interacted with the high endothelial cells in Peyer's patches, although it did not affect the rolling flux (Figures 3C and 3D). The number of firmly adherent cells was also drastically diminished in the *AOC3*$^{-/-}$ animals when compared to the wt controls (Figure 3E).

It is not possible to analyze transmigration in the intravital model because lymphocytes only poorly transmigrate in surgically exposed lymph nodes (von Andrian and Mempel, 2003). Therefore, we further addressed the role of AOC3 in lymphocyte traffic by using short-term homing experiments. We fluorescently labeled lymphocytes isolated from spleen and lymph nodes of wt animals and injected them intravenously into recipient animals. After a 4 hr recirculation time, the number of adoptively-transferred lymphocytes in the peripheral and mesenteric lymph nodes, Peyer's patches, and spleen was determined by FACS analyses. When compared to wt recipients, the homing of lymphocytes in the *AOC3*-deficient animals was significantly less efficient in MLN and spleen, and a trend of impaired homing was seen also in PP and PLN (Figure 3F). We thus conclude that in addition to PMN extravasation, AOC3 also contributes to the physiological patrolling of lymphocytes through lymphoid organs.

AOC3 is not expressed on leukocytes (Salmi and Jalkanen, 1992), but the loss of SSAO activity could cause indirect effects on the expression of homing-associated molecules on these cells. However, flow cytometric analyses revealed that expression of L-selectin, P-selectin glycoprotein ligand 1, $\alpha 4\beta 7$ integrin, CD18, and CD44 on peripheral blood leukocytes in AOC3-deficient animals was indistinguishable from that seen in controls (data not shown). Because AOC3 activity results in Schiff-base formation and Schiff bases are known to stabilize L-selectin ligand interaction (Puri and Springer, 1996), we measured the function of L-selectin in *AOC3* knockouts. The results showed that mAb MEL-14 against mouse L-selectin significantly inhibited the rolling flux of leukocytes in the inflamed cremaster both in wt and *AOC3*-deficient animals (Figure 4D). Anti-L-selectin blockade also diminished leukocyte rolling in the Peyer's patches of *AOC3*$^{-/-}$ mice (data not shown). These data show that the function of L-selectin appears not to be affected by AOC3. Absence of AOC3 did not cause any immunohistochemically detectable change in the expression of endothelial adhesion molecules P-selectin, E-selectin, PNAd, MAdCAM-1, ICAM-1, VCAM-1, or CD31 either in Peyer's patches or in inflamed vessels of cremaster (Figures 2A, 2B, 3A, and 3B and data not shown). Thus, changes in leukocytes, hemodynamic parameters (Tables 1 and 2), or in other adhesion molecules studied do not account for the marked aberrations of the leukocyte-endothelial contacts observed in *AOC3*$^{-/-}$ mice.

AOC3$^{-/-}$ Mice Show Diminished Leukocyte Influx in Autoimmune Diabetes and Peritonitis

To compare our real-time imaging experiments showing a crucial role for AOC3 in the extravasation cascade with disease models in vivo, we finally studied immune responses in the presence and absence of AOC3. The baseline proliferation and CD3-triggered proliferation of splenocytes were indistinguishable between the two genotypes (Figure 5A). Immunizations of the wt and *AOC3*$^{-/-}$ animals with a T cell-dependent antigen ovalbumin (OVA) or with a T cell-independent antigen lipopolysaccharide (LPS) yielded similar lymphocyte proliferation responses (Figure 5A). The production of OVA-specific antibodies of IgG subclasses or LPS-specific IgM antibodies in response to these immunizations also did not differ significantly between the genotypes (Figure 5B). The total serum immunoglobulin levels of IgG, IgM, and IgA subclasses in unchallenged *AOC3*$^{+/+}$

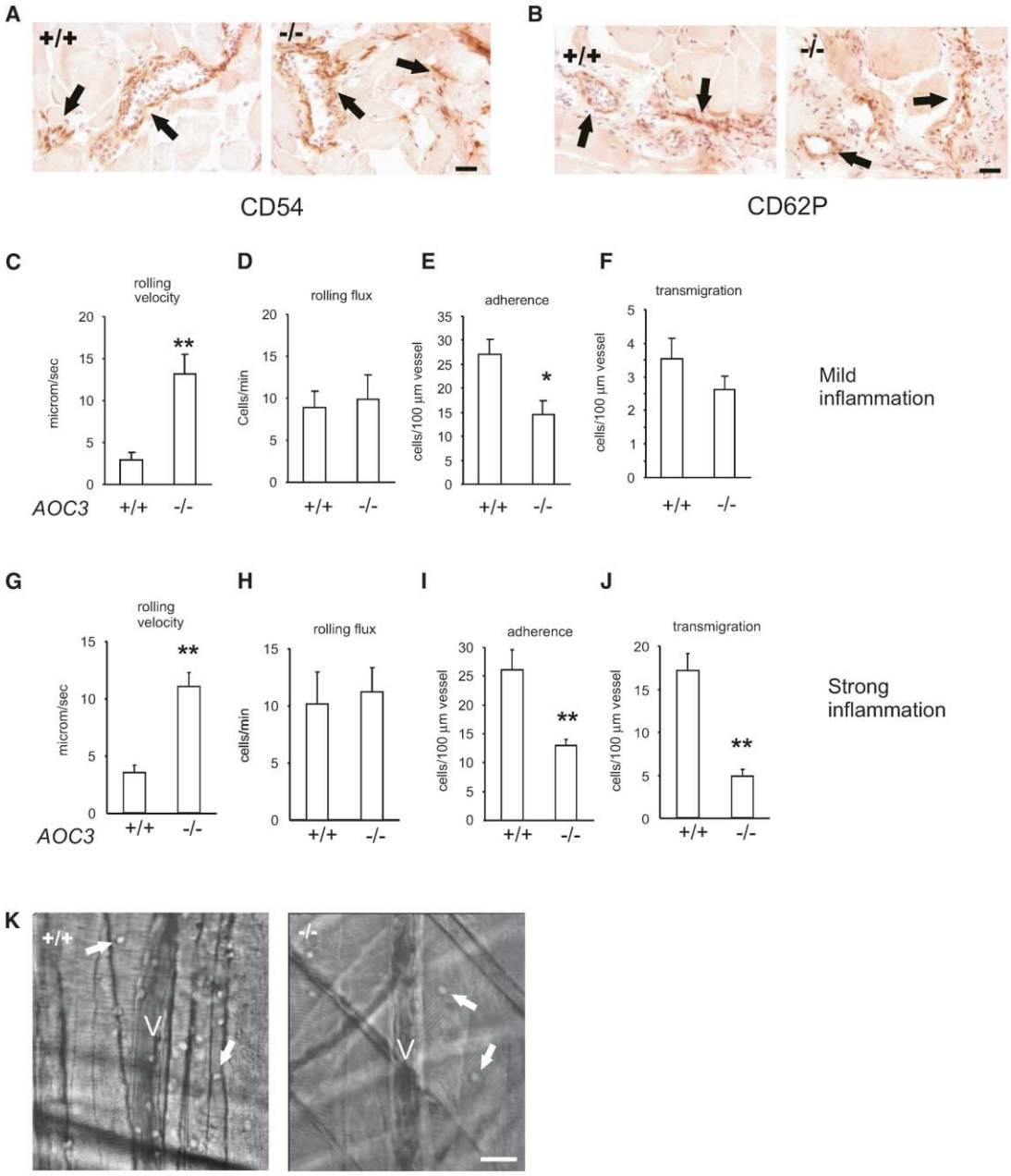

Figure 2. AOC3 is Needed for Rolling, Firm Adhesion, and Transmigration in Inflamed Vasculature

(A and B) The morphology of vessels and expression of ICAM-1/CD54 (A) and P-selectin/CD62P (B) in the cremaster of wild-type (+/+) and *AOC3*$^{-/-}$ animals was analyzed by using immunohistochemical stainings. Positive reactivity is visible as brown precipitates. Arrows point to representative vessels. Bars, 50 μm.

(C–J) The velocity of rolling cells (C and G), the number of rolling cells (D and H), the number of firmly bound cells (E and I), and the number of transmigrated cells (F and J) was determined by using intravital videomicroscopy in wt and *AOC3*$^{-/-}$ mice. The vasculature was mildly (C–F) or strongly (G–J) inflamed with intrascrotal TNF-α injections (0.5 μg for 3 hr and 1.5 μg for 6 hr, respectively). The results are mean ± SEM of 110–170 vessels from five different animals in each group. *p value < 0.05; **p value < 0.01. The real-time images from a representative wt and *AOC3*$^{-/-}$ vessel are shown in the supplemental videos.

(K) Still images from the strong inflammation model. Leukocytes (some indicated by white arrows) emigrating from a venule (V) in a cremaster of *AOC3*$^{+/+}$ and *AOC3*$^{-/-}$ animals are shown. Bar, 25 μm.

animals were 1.8 ± 0.2, 0.3 ± 0.01, and 2.9 ± 0.2 mg/ml, and those in *AOC3*$^{-/-}$ animals 2.1 ± 0.3, 0.3 ± 0.03 and 2.0 ± 0.2 mg/ml, respectively (n = 10 for both genotypes, difference in sIgA reached statistical significance [$p < 0.01$]). These data suggest that AOC3 is not essential for lymphocyte proliferation or antibody responses, although there may be minor changes in the total concentrations of serum immunoglobulins.

To study whether absence of AOC3 would compromise the antimicrobial defense, mice were challenged

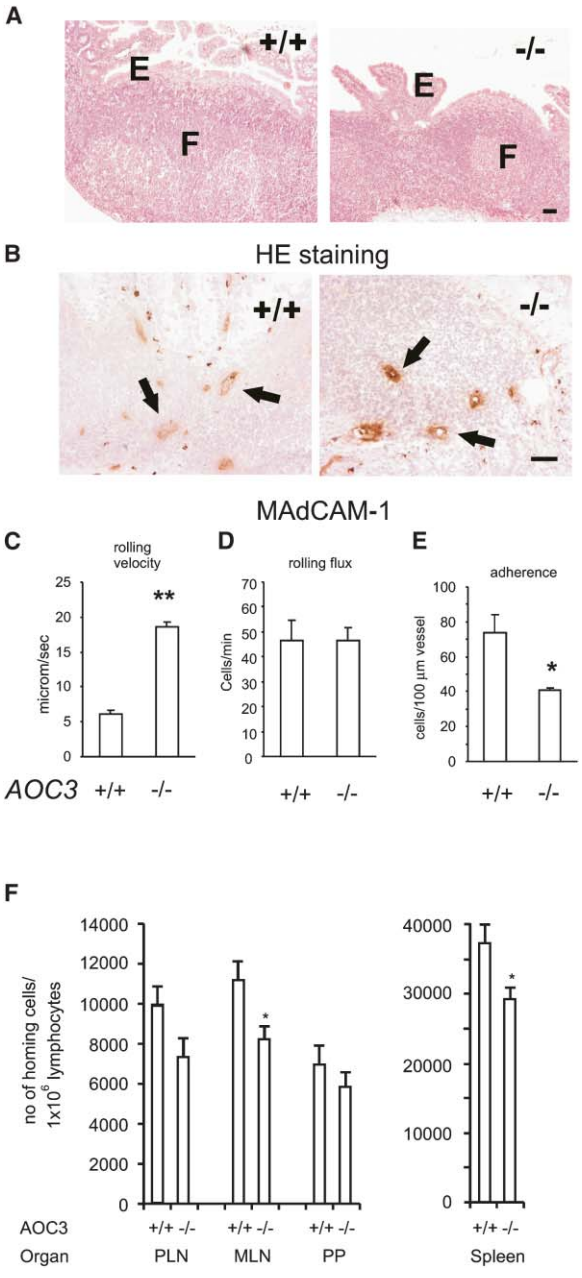

Figure 3. AOC3 Mediates Lymphocyte Traffic in Lymphoid Tissues

(A and B) The morphology of Peyer's patches ([A], hematoxylin-eosin staining) and expression of mucosal addressin MAdCAM-1 ([B], immunohistochemical staining) in wt (+/+) and *AOC3*$^{-/-}$ animals was analyzed. E, epithelium of gut; F, lymphoid follicle; and black arrows point to representative positive high endothelial venules. Bar, 50 μm.

(C–E) The velocity of rolling cells (C), the number of rolling cells (D), and the number of firmly bound cells (E) was determined by using intravital videomicroscopy and fluorescently labeled cells in wt and *AOC3*$^{-/-}$ mice. The results are mean ± SEM of 99–131 vessels from five different animals in each group. *p value < 0.05; **p value < 0.01.

(F) Short-term homing assays reveal impaired lymphocyte traffic in *AOC3*$^{-/-}$ mice. Fluorescently-labeled donor cells were administered intravenously into recipient animals, and the number of cells that have homed into peripheral lymph nodes (PLN), mesenteric lymph node (MLN), Peyer's patches (PP), and spleen was determined 4 hr later by isolating the cells from lymphoid organs of the recipient animals and running one million cells per sample through FACS and recording the number of fluorescently-labeled cells among this population. *p value < 0.05; n = 7/genotype.

with virulent Yersinia enterocolitica serotype O:8, a gram-negative enteropathogen. Mice were inoculated intragastrically with different doses of bacteria, and the survival of the animals was followed. The symptoms of the disease appeared at the same time scale in both *AOC3*$^{-/-}$ and wt littermates, and there were no marked differences in the survival between the two genotypes (Figure 5C). Thus, absence of AOC3 does not impair an immune response against a life-threatening microbial infection.

The contribution of AOC3 in lymphocyte homing into an area of nonbacterial inflammation was studied in autoimmune diabetes. In a transgenic transfer model, intravenous administration of OVA-specific, CD8-positive T cells from the T cell receptor-transgenic OT-I animals into mice expressing the OVA antigen specifically in pancreatic islets under control of rat insulin promoter (RIPmOVA mice) leads to a fulminant insulitis and diabetes (Kurts et al., 1996). We used either *AOC3*$^{-/-}$RIPmOVA or *AOC3*$^{+/+}$RIPmOVA littermates as recipients in this model. The outcome of this lymphocyte-dependent disease was notably different, because only 17% of the animals lacking AOC3 died of the diabetes, whereas 44% of the AOC3-positive controls succumbed to the disease during the 10 day follow up (Figure 5D). More detailed analyses showed that there were no marked differences between the groups in the blood glucose concentrations during days 4–10 of disease development (data not shown). However, histological analyses of pancreata at day 5 revealed a trend of decrease in the numbers of infiltrating lymphocytes in the islets of AOC3$^{-/-}$ animals when compared to wt littermates (the insulitis scores were 1.48 ± 0.26 [mean ± SEM; 4 animals, 204 islets] and 1.81 ± 0.08, [3 animals, 153 islets], respectively).

Finally, as an acute model of noninfectious inflammation, a cytokine-induced peritonitis was used. *AOC3*$^{-/-}$ animals showed a 50% reduction in the number of infiltrating leukocytes when compared to the wt controls 6 hr after the induction of the inflammation by an intraperitoneal injection of TNF-α (Figure 5E). Together, the inflammation models suggest that AOC3 is needed in vivo to mount adequate inflammatory reactions in response to nonmicrobial stimuli.

Discussion

We show here that a cell-surface amine oxidase controls leukocyte traffic in vivo. Absence of AOC3 impairs the capacity of lymphocytes and PMN to interact with vascular endothelium and manifests as highly increased rolling velocity, diminished firm adhesion, and reduced transmigration. Deletion of AOC3 inhibits constitutive lymphocyte recirculation and the inflammatory response in diseases like autoimmune diabetes and peritonitis. Our data provide direct physiological evidence for a new concept that ectoenzymes regulate the formation of inflammatory infiltrate in vivo.

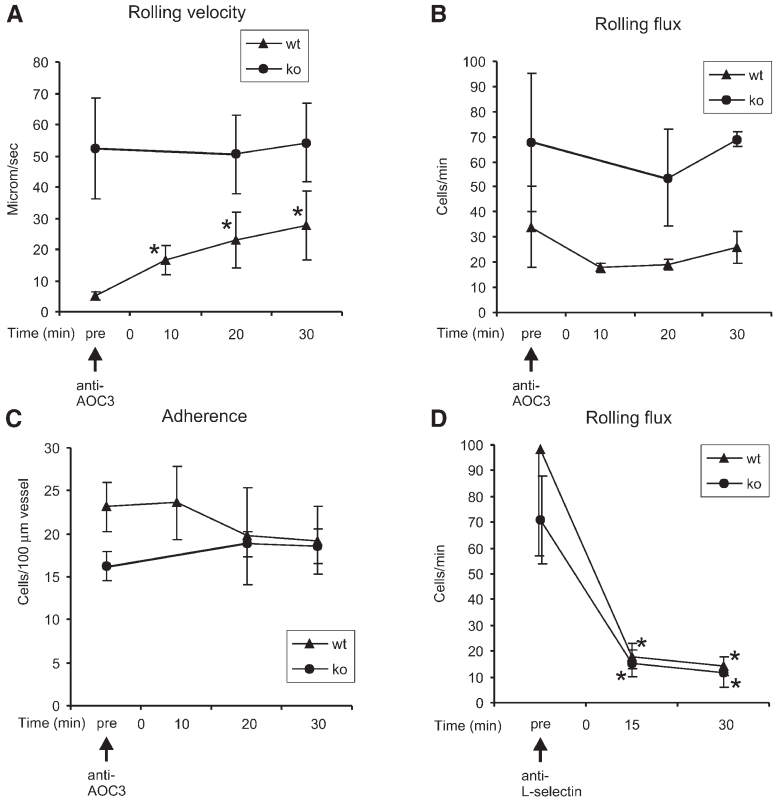

Figure 4. Anti-AOC3 mAbs Inhibit Leukocyte-Endothelial Contacts in the Wt Animals and the Function of L-Selectin Is Not Disturbed in the Absence of AOC3

(A–C) The vasculature in creamaster of *AOC3*$^{+/+}$ and *AOC3*$^{-/-}$ animals was inflamed by a 6 hr intrascrotal TNF-α exposure (strong inflammation model). Then, the velocity of rolling cells (A), the number of rolling cells (B), and the number of firmly adherent cells (C) was determined just before (pre) and at indicated time points (10, 15, and 30 min) after giving an intravenous bolus of anti-AOC3 mAb 7-106 (arrow) by using intravital videomicroscopy. The results are mean ± SEM of 13–31 vessels from five different animals in both groups. *p value < 0.05 (pre versus the indicated time point, n = 5).

(D) The vasculature in creamaster of *AOC3*$^{+/+}$ and *AOC3*$^{-/-}$ animals was inflamed by a 3 hr intrascrotal TNF-α exposure (mild inflammation model). Then, the number of rolling cells (mean ± SEM) was determined just before (pre) and at indicated time points (15 and 30 min) after giving an intravenous bolus of anti-L selectin mAb MEL-14 (arrow) by using intravital videomicroscopy. The results are mean ± SEM of 24–30 vessels from four different animals in both groups. *p value < 0.05 (pre versus the indicated time-point, n = 4).

SSAOs were enzymatically identified in the 1950s, but their physiological functions have remained enigmatic (Jalkanen and Salmi, 2001; Klinman and Mu, 1994; Yu et al., 2003). In man, four genes encoding SSAO enzymes have been described: a diamine oxidase AOC1 (Chassande et al., 1994), two splice variants of a retina-specific SSAO (AOC2) (Imamura et al., 1998), an apparent SSAO pseudogene (Cronin et al., 1998), and AOC3 (Smith et al., 1998; Zhang and McIntire, 1996), and homologous genes are present in the mouse genome. Our findings that deletion of AOC3 completely abolishes all detectable SSAO activity in mice show that AOC3 is the dominant SSAO in these animals.

SSAO catalyze the general reaction $R - CH_2 - NH_2 + H_20 + O_2 \rightarrow R - CHO + NH_3 + H_2O_2$ (Jalkanen and Salmi, 2001; Klinman and Mu, 1994). Although the identity of physiological substrates of SSAO remains controversial, either soluble amines (methylamine or aminoacetone) or a suitable cell-surface molecule containing free NH2 groups can likely serve as an AOC3 ligand/substrate (O'Sullivan et al., 2003; Salmi et al., 2001; Yu et al., 2003). Thus, in the absence of AOC3, the substrates are not deaminated and no end products with potential biological functions are produced. Moreover, the formation of the covalent but transient Schiff base (Klinman and Mu, 1994) between endothelial SSAO and its potential substrate(s) on leukocytes does not take place in *AOC3*$^{-/-}$ animals. This can physically result in diminished contacts between leukocytes and vascular wall, and it also prevents conversion of leukocyte surface amines into adhesive aldehyde compounds. Direct function of endothelial AOC3 is likely to be crucial in this context, because we did not observe any phenotypic changes related to homing-associated molecules other than AOC3 either on leukocyte or endothelial cell surface. However, we do not rule out indirect AOC3-mediated signaling effects either, because they can modulate the activity of the tested or other known or unknown adhesion molecules in a way not detectable by immunostainings. We thus believe that either signaling, direct adhesive functions of AOC3, or their combination can mechanistically explain the observed adhesion-defective phenotype of *AOC3*$^{-/-}$ animals.

Rolling, firm adhesion, and transmigration all appear to be affected in *AOC3*$^{-/-}$ animals. Because extravasation is a multistep process, the defects in adhesion and diapedesis could be secondary to diminished interactions at an earlier step(s) or be caused by an independent function of AOC3 at multiple steps. Our quantitative analyses of conversion of rolling to firm adhesion and of adhesion to transmigration are suggestive for the latter possibility. AOC3 is important in regulating the velocity of rolling cells. Traditionally, slow (AOC3-mediated) rolling is thought to be critical for subjecting leukocytes to chemotactic activation and stable adhesion. On the endothelial surface in vivo, to our knowledge, only E-selectin has been reported to share the braking function with AOC3. In the E-selectin$^{-/-}$ animals, the average rolling velocity is five to six times faster than in controls but, in contrast to AOC3-deficient animals, the rolling flux is increased and the transmigratory response is normal (Kunkel and Ley, 1996). Blockade of $\alpha 4\beta 7$ integrin on lymphocytes also diminishes the rolling velocity, suggesting that its endothelial ligands are also involved in braking. Our data suggest that AOC3 also contributes significantly to firm adhesion, because 50%

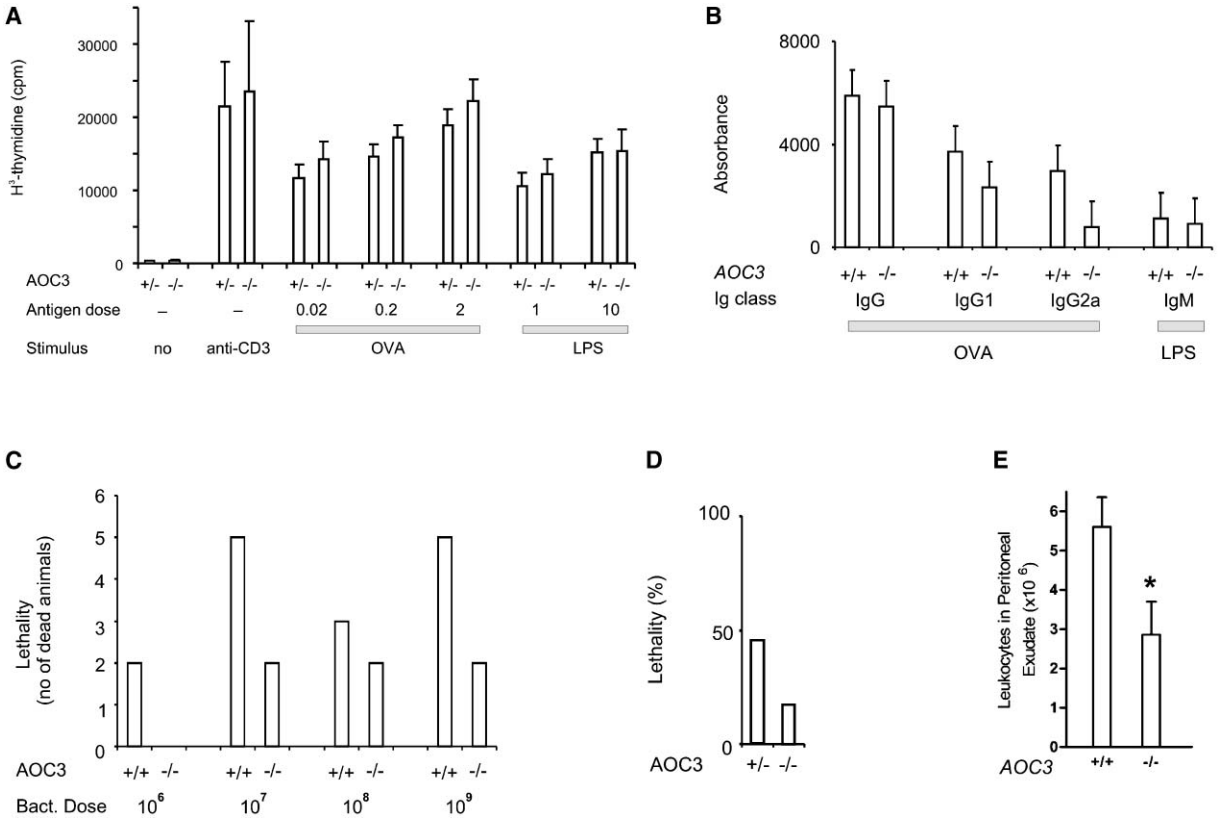

Figure 5. Absence of AOC3 Inhibits Inflammation in Autoimmune Diabetes and in Chemically Induced Peritonitis but Does Not Compromise Antimicrobial Responses

(A and B) $AOC3^{+/+}$ and $AOC3^{-/-}$ animals were immunized subcutaneously with ovalbumin (OVA) and intraperitoneally with lipopolysaccharide (LPS), and antigen-specific lymphocyte proliferation (A) and antibody responses (B) were measured. Proliferation of lymphocytes in unchallenged animals was also determined in the absence of any stimulus (no) or in the presence of triggering anti-mouse CD3 mAb. The results are mean ± SEM of at least 5–15 different animals (each analyzed in triplicate) in each group.

(C) Yersinia bacteria were inoculated intragastrically in the mice at the indicated doses, and the viability of the animals was followed for 10 days. The results are from six animals per group.

(D) Autoimmune diabetes was induced to RIPmOVA-transgenic animals expressing or not expressing AOC3 by transfer of OVA-specific transgenic, CD8-positive T cells. The survival of animals ($AOC3^{-/-}$, n = 12 and $AOC3^{+/+}$, n = 18) was followed for 10 days.

(E) Wt and $AOC3^{-/-}$ animals were subjected to TNF-α induced chemical peritonitis, and the number of cells in the lavage fluid were determined. The results are mean ± SEM of nine wt and six $AOC3^{-/-}$ animals. *p value < 0.05; **p value < 0.01.

fewer stably adherent cells were observed in $AOC3^{-/-}$ animals. The data also suggest that AOC3 mediates diapedesis independently of its effects on earlier steps of the cascade. This is in line with earlier in vitro studies showing that anti-AOC3 mAbs and SSAO inhibitors diminish transmigration (Koskinen et al., 2004; Lalor et al., 2002). Based on the antibody inhibition experiments, CD31, CD99, JAM-A, and JAM-C have been thought to be important for transmigration (Johnson-Leger et al., 2002; Muller et al., 1993; Ostermann et al., 2002; Schenkel et al., 2002). However, data with JAM-A are conflicting (Lechner et al., 2000; Schenkel et al., 2004), and so far the only evidence for CD31 has been provided in gene-targeted animals (Dangerfield et al., 2002; Duncan et al., 1999; Thompson et al., 2001). Most importantly, AOC3 is apparently needed for normal leukocyte traffic in vivo, because in AOC3-deficient animals we observed >70% reduction in the absolute numbers of extravasated cells in intravital studies.

Deletion of AOC3 caused an impairment of lymphocyte homing. This manifested as diminished rolling and firm adhesion of leukocytes in Peyer's patches in intravital videomicroscopy and as significantly impaired homing of adoptively transferred lymphocytes into mesenteric lymph nodes and spleen. However, absence of AOC3 resulted in no obvious defect in immune surveillance, lymphocyte proliferation, or antibody responses under specific pathogen-free conditions. The mortality of $AOC3^{-/-}$ animals challenged with gram-negative bacteria was not higher than that of similarly infected wt littermates. Nevertheless, both the development of lymphocyte-dependent autoimmune diabetes and acute peritoneal inflammation were inhibited in the absence of AOC3. We interpret these data so that when the body is confronted by a massive life-threatening microbial attack, multiple, different pathways are activated in parallel to mount a maximal defense response involving all types of cells belonging to the innate immunity. In this case, the other endothelial adhesion molecules can probably compensate for the loss of AOC3. In contrast, when a more innocent nonbacterial danger signal is encountered, the endothelial activation is more limited, and the individual role of AOC3 is readily discernible.

As an enzyme, AOC3 opens new venues for develop-

ment of antiadhesive therapeutics. Small molecule inhibitors of SSAO are available (Koskinen et al., 2004), and they should avoid many of the problems encountered when exploiting function-blocking mAb in clinical trials. Moreover, AOC3 is mainly intracellular under normal conditions, but its luminal expression is induced upon inflammation (Jaakkola et al., 2000). Thus, blockade of AOC3 should have preferential effects at inflammatory sites. The facts that deletion of AOC3 did not cause any overt macroscopic phenotype, and did not compromise normal T- or B cell-dependent lymphocyte activation or antibacterial defense strongly support the feasibility of this molecule as a therapeutic target. Nevertheless, because the lack of AOC3 inhibited lymphocyte homing, potential side effects of AOC3 targeting need careful evaluation. Collectively, these data suggest that AOC3 may play a more important role in inappropriate inflammatory conditions, like in ischemia-reperfusion injury or in autoimmune diseases like rheumatoid arthritis or autoimmune diabetes, than in physiologic recirculation or microbial infections. Significant impairment of leukocyte extravasation in our noninfectious inflammation models in vivo in the absence of AOC3 predicts good potential for new antiadhesive therapies targeting AOC3.

In conclusion, the *AOC3*$^{-/-}$ animals are the first direct evidence that an ectoenzyme is needed for the leukocyte traffic under physiological conditions in vivo. Enzymatic control of leukocyte traffic provides a significant alteration to the currently accepted multistep model of leukocyte extravasation cascade.

Experimental Procedures

Generation of Homozygous *AOC3*$^{-/-}$ Mice

AOC3 targeting vector was constructed by subcloning a 2.7 kb 5′ KpnI – HindIII and a 2.65 kb 3′ SalI – AflII fragment of 129X1 genomic DNA flanking base pairs 4502–5067 of mouse *AOC3* (AF078705) into the pGT-N29 vector (New England Biolabs, Beverly, MA) at either end of a Neo^r cassette.

AB2.2-prime embryonic stem cells (Lexicon Genetics, Woodlands, TX) were electroporated with the AOC3 targeting construct and selected for G418 resistance at the CMB/MouseCamp (Karolinska Institute, Sweden). Clones with homologous recombination (6 out of 577) were selected by PCR with a common 3′ oligo CS-6: 5′-GCTGTGAGCTGTGCTCAGAT-3′, a Neo^r-specific oligo CS-7: 5′-CGAGATCAGCAGCCTCTGTT-3′, and a wt AOC3 oligo CS-11: 5′-GGTATTCTATCAAGGCCGTTAC-3′.

Blastocyst injections and transfers were performed at the CMB/MouseCamp. 11 chimeric mice were obtained and bred to 129S6 mice. Germline transmission was identified by PCR analysis of genomic DNA with Neo^r-specific oligos CS-23: 5′-GGCTGCTGATCTCG TTCTTC-3′ and CS-24: 5′-TCTGGATTCATCGACTGTGG-3′. Homozygous mice were then obtained by intercrossing and identified with the Neo^r specific PCR together with a PCR that is specific for the wt AOC3 allele (CS-21: 5′-GCCCACAAGGAAGAAGACAC-3′ and CS-22: 5′-CAAACACCAGGGACAGAACC-3′). The initial recombination events and mouse zygosity screens were confirmed by Southern blotting DraIII or KpnI digested genomic DNA with an AOC3-specific PCR-generated probe (CS-5: 5′-GACCCAGAGAGCACTCTGAT-3′ and CS-9: 5′-CTCTCTGTCCAACACAGGAC-3′). The null mutation was backcrossed onto the 129S6 background three times before intercrossing to generate homozygous null mice. All mice were handled in accordance with the institutional animal care policy of the University of Turku.

Histological Analyses

Organs were removed, fixed in 10% formaldehyde overnight, dehydrated, embedded in paraffin, sectioned, and stained with hematoxylin and eosin. For immunohistology, frozen sections were stained with monoclonal anti-mouse AOC3 antibodies (7-88, 7-106, or 7-188) at 50 μg/ml and peroxidase-conjugated rabbit anti-rat immunoglobulins. Other mAbs against endothelial adhesion molecules were used in a similar fashion. Digital photomicrographs were created with AnalySIS version 3.00 software (Soft Imaging System GmbH).

Measurement of SSAO Activity

Serum was separated from blood drawn from the heart. Tissue samples were cut into small pieces and lysed in an equal volume of lysis buffer (PBS and 0.2% Triton X-100). Amine oxidase activity was assayed radiochemically by using 2 μM [7-^{14}C]-benzylamine hydrochloride (Amersham) as a substrate. Alternatively, fluorometric determination of the reaction product H_2O_2 was assayed by using 1 mM unlabeled substrates, adipocyte lysate, and Amplex Red reagent (Salmi et al., 2001).

Intravital Videomicroscopy

The procedures were adapted from Ley et al. (1995). In brief, mice were anesthetized by ketamine and xylazine, and TNF-α was injected intrascrotally for inducing mild (0.5 μg, 3 hr) or strong (1.5 μg, 6 hr) inflammation. Cannula were inserted into the jugular vein, and the cremaster muscle was dissected free and pinned on a special microscopic stage. The tissue was kept moist and warm by continuous superfusion with a buffered salt solution. An Olympus microscope equipped with a long-distance water immersion objective and CCD camera was used to record the experiment on a digital video recorder. The centerline red blood cell velocity was measured by using a commercial velocimeter (CircuSoft) fitted to the microscope. All other parameters were measured offline from the videos. The rolling flux is defined as the number of leukocytes rolling in close contact to vessel wall across a fixed line during 1 min. The rolling velocity of cells was determined by analyzing the time needed for cells to roll through a 100 μm segment of the vessel. A leukocyte was scored firmly adherent if it was stably stuck to the endothelial cells for at least 30 s and transmigrated if it was in the perivenular tissue within 50 μm of the 100 μm vessel segment under observation. The Newtonian wall shear rates (γ) were approximated as $\gamma = 2.12 \times 8 \times V_b/d$ (s^{-1}), where 2.12 is an empirical correction factor, d is the mean diameter of the vessel, and V_b is the mean blood flow velocity (obtained by multiplying the centerline red blood cell velocity with an empirical factor of 0.625), as described (Kunkel and Ley, 1996; von Andrian et al., 1992).

For visualizing lymphocyte interactions with HEV, gut was exteriorized from a midline incision and a Peyer's patch was gently overlaid with a coverslip (Bargatze et al., 1995). The animals then got an intravenous bolus of nuclear stain Rhodamine 6G. Leukocyte-endothelial interactions in superficial HEV were observed by using stroboscopic epifluorescence and the CCD camera. Centerline velocity was directly measured from the fastest noninteracting cells, and the other parameters were counted as described above.

In certain assays, a bolus (100 μg) of function-blocking anti-AOC3 mAb 7-106 or anti-L-selectin mAb MEL-14 was administered intravenously to the animals. The whole experiment was recorded by using intravital videomicroscopy, and the leukocyte-endothelial interactions were analyzed just before the mAb administration (pre) and at 10, 20, and 30 min or at 15 and 30 min after the antibody injection.

Lymphocyte Counts, Phenotype, and Short-Term Homing

Lymphocyte suspensions were prepared from the peripheral lymph nodes (only axillary and inguinal nodes), mesenteric lymph node, Peyer's patches, thymus, and spleen of age-matched *AOC3*$^{+/+}$ and *AOC3*$^{-/-}$ mice by using mechanical teasing through a steel mesh. Erythrocytes were lysed from the spleen by a brief hypotonic lysis. The number of Peyer's patches in each animal was determined macroscopically. The lymphocyte counts were done by microscopic counting of the Trypan blue-stained cells in Neubauer chambers.

The phenotype of tissue-derived and blood leukocytes was determined by immunofluorescence stainings by using monoclonal antibodies against CD4, CD8, B220, and against various leukocyte adhesion molecules. The cells were analyzed by FACS.

For homing experiments, pooled lymphocytes from peripheral lymph nodes, mesenteric lymph node, and spleen were fluorescently labeled by a 30 min incubation with CMFDA-AM. After washings,

20×10^6 cells in 200 μl RPMI were injected intravenously into the tail vein (seven animals per group). After a 4 hr recirculation time, the animals were killed and lymphocyte suspensions were prepared from secondary lymphoid organs (peripheral lymph nodes, mesenteric lymph node, Peyer's patches, and spleen). Thereafter one million lymphocytes per sample were run through a FACS machine and the number of fluorescently labeled cells within this population (i.e., the number of donor cells that have homed into the given organ of the recipient animal) was determined.

Immunizations with OVA and LPS

The animals were immunized subcutaneously with purified OVA (0.2 mg/200 μl) in CFA and intraperitoneally with LPS (10 μg in 100 μl PBS). After 2 weeks, splenocytes were isolated and subjected to standard thymidine incorporation tests. Base-line proliferation in unimmunized animals was determined in the same manner without any stimulation or in the presence of triggering anti-CD3 mAb. Antigen-specific Ig titers were assayed from sera by using microtiter plates coated with OVA or LPS and peroxidase-conjugated anti-mouse IgG subclass or IgM-specific reagents in an ELISA, essentially as described (Boyle et al., 1997). Concentrations of major serum immunoglobulin isotypes (sIgG, sIgM, and sIgA) in normal, unimmunized animals were determined by using quantitative sandwich ELISAs (Bethyl Laboratories) and fourth order polynomial curve fitting programs.

Yersinia Infections

Serial 10-fold dilutions were prepared from a suspension of *Yersinia enterocolitica* serotype O:8 strain 8081 (Portnoy et al., 1981). 100 μl of suspensions containing approximately 10^7, 10^8, 10^9, or 10^{10} cfu/ml were given to groups of three mice intragastrically with a 20 gauge stainless steel ball-tipped catheter. The health status and deaths of mice were followed daily for 10 days. The experiment was repeated twice (total six animals/group).

Transfer Model of Autoimmune Diabetes

OT-1 and RIPmOVA transgenic mice and the T cell transfer model for inducing lymphocyte-dependent autoimmune diabetes have been previously described (Kurts et al., 1996). *AOC3*$^{-/-}$ mice were crossed with C57BL/6JBom wt animals and then backcrossed with this line for five generations. These mice were then crossed with the RIPmOVA (C57BL/6) animals to produce *AOC3*$^{-/-}$RIPmOVA and *AOC3*$^{+/+}$RIPmOVA (C57BL/6 (N6)) mice. The presence of both AOC3 and RIP genes was followed by using specific PCRs. CD8-positive T cells specific for OVA were isolated from the lymph nodes of OT-I animals. 2×10^6 OT-I cells (H2K^b-SIINFEKL-tetramer positive) were then intravenously injected to *AOC3*$^{+/+}$RIP-mOVA and *AOC3*$^{-/-}$ RIPmOVA littermates, and the animals were followed for 10 days for the development of diabetes. The blood glucose was measured at days 4, 6, 8, and 11 by using Glucotest. For histological analyses of insulitis, animals were killed on day 5 (during the early development of the insulitis). The numbers of islet-infiltrating lymphocytes were scored blindly in a semiquantitative manner from hematoxylin eosin-stained paraffin sections cut from the pancreata as follows: score 0, no islet-infiltrating lymphocytes; score 1, peri-islet infiltrate; score 2, infiltrating cells occupying $<$50% of the islet area; and score 3, infiltrating cells occupying over 50% of the islet. Mean insulitis values represent the frequency of islets in these categories (Hänninen et al., 1998). In these experiments, four *AOC3*$^{-/-}$ RIPmOVA and three *AOC3*$^{+/+}$RIPmOVA animals were used, and the number of analyzed islets was 59–80 in each animal.

Peritonitis

50 ng of TNF-α in 1 ml of PBS was injected intraperitoneally into *AOC3*$^{-/-}$ and wt animals. 6 hr later, the mice were killed, the peritoneal cavity was lavaged, and the numbers of leukocytes were counted.

Statistics

Parametric and nonparametric variables between the *AOC3*$^{+/+}$ and *AOC3*$^{-/-}$ groups were compared with Student's t test and chi-square tests, respectively.

Acknowledgments

We thank Ms. Kira Stolen, Marika Merinen, Suvi Nevalainen, Maritta Pohjansalo, and Sari Mäki for expert technical help and Anne Sovikoski-Georgieva for secretarial assistance. The study was supported by the Finnish Academy, Technology Development Centre of Finland, Finnish Diabetes Research Foundation, European Union (QLG1-CT-1999-00295), and Sigrid Juselius Foundation. One of the authors (S.J.) has a financial interest in a company that works with AOC3.

Received: May 13, 2004
Revised: November 24, 2004
Accepted: December 1, 2004
Published: January 25, 2005

References

Bargatze, R.F., Jutila, M.A., and Butcher, E.C. (1995). Distinct roles of L-selectin and integrins α4β7 and LFA-1 in lymphocyte homing to Peyer's patch-HEV in situ: the multistep model confirmed and refined. Immunity *3*, 99–108.

Boyle, J.S., Silva, A., Brady, J.L., and Lew, A.M. (1997). DNA immunization: induction of higher avidity antibody and effect of route on T cell cytotoxicity. Proc. Natl. Acad. Sci. USA *94*, 14626–14631.

Chassande, O., Renard, S., Barbry, P., and Lazdunski, M. (1994). The human gene for diamine oxidase, an amiloride binding protein. Molecular cloning, sequencing, and characterization of the promoter. J. Biol. Chem. *269*, 14484–14489.

Cronin, C.N., Zhang, X., Thompson, D.A., and McIntire, W.S. (1998). cDNA cloning of two splice variants of a human copper-containing monoamine oxidase pseudogene containing a dimeric *Alu* repeat sequence. Gene *220*, 71–76.

Dangerfield, J., Larbi, K.Y., Huang, M.T., Dewar, A., and Nourshargh, S. (2002). PECAM-1 (CD31) homophilic interaction up-regulates alpha6beta1 on transmigrated neutrophils in vivo and plays a functional role in the ability of alpha6 integrins to mediate leukocyte migration through the perivascular basement membrane. J. Exp. Med. *196*, 1201–1211.

Dejana, E. (2004). Endothelial cell-cell junctions: happy together. Nat. Rev. Mol. Cell Biol. *5*, 261–270.

Duncan, G.S., Andrew, D.P., Takimoto, H., Kaufman, S.A., Yoshida, H., Spellberg, J., Luis de la Pompa, J., Elia, A., Wakeham, A., Karan-Tamir, B., et al. (1999). Genetic evidence for functional redundancy of Platelet/Endothelial cell adhesion molecule-1 (PECAM-1): CD31-deficient mice reveal PECAM-1-dependent and PECAM-1-independent functions. J. Immunol. *162*, 3022–3030.

Hänninen, A., Jaakkola, I., and Jalkanen, S. (1998). Mucosal addressin is required for the development of diabetes in nonobese diabetic mice. J. Immunol. *160*, 6018–6025.

Imamura, Y., Noda, S., Mashima, Y., Kudoh, J., Oguchi, Y., and Shimizu, N. (1998). Human retina-specific amine oxidase: genomic structure of the gene (AOC2), alternatively spliced variant, and mRNA expression in retina. Genomics *51*, 293–298.

Jaakkola, K., Nikula, T., Holopainen, R., Vähäsilta, T., Matikainen, M.-T., Laukkanen, M.-L., Huupponen, R., Halkola, L., Nieminen, L., Hiltunen, J., et al. (2000). In vivo detection of vascular adhesion protein-1 in experimental inflammation. Am. J. Pathol. *157*, 463–471.

Jalkanen, S., and Salmi, M. (2001). Cell surface monoamine oxidases: enzymes in search of a function. EMBO J. *20*, 3893–3901.

Johnson-Leger, C.A., Aurrand-Lions, M., Beltraminelli, N., Fasel, N., and Imhof, B.A. (2002). Junctional adhesion molecule-2 (JAM-2) promotes lymphocyte transendothelial migration. Blood *100*, 2479–2486.

Klinman, J.P., and Mu, D. (1994). Quinoenzymes in biology. Annu. Rev. Biochem. *63*, 299–344.

Koskinen, K., Vainio, P.J., Smith, D.J., Pihlavisto, M., Yla-Herttuala, S., Jalkanen, S., and Salmi, M. (2004). Granulocyte transmigration through endothelium is regulated by the oxidase activity of vascular adhesion protein-1 (VAP-1). Blood *103*, 3388–3395.

Kunkel, E.J., and Butcher, E.C. (2002). Chemokines and the tissue-specific migration of lymphocytes. Immunity *16*, 1–4.

Kunkel, E.J., and Ley, K. (1996). Distinct phenotype of E-selectin-deficient mice. E-selectin is required for slow leukocyte rolling in vivo. Circ. Res. *79*, 1196–1204.

Kurts, C., Heath, W.R., Carbone, F.R., Allison, J., Miller, J.F., and Kosaka, H. (1996). Constitutive class I-restricted exogenous presentation of self antigens in vivo. J. Exp. Med. *184*, 923–930.

Lalor, P.F., Edwards, S., McNab, G., Salmi, M., Jalkanen, S., and Adams, D.H. (2002). Vascular adhesion protein-1 mediates adhesion and transmigration of lymphocytes on human hepatic endothelial cells. J. Immunol. *169*, 983–992.

Lechner, F., Sahrbacher, U., Suter, T., Frei, K., Brockhaus, M., Koedel, U., and Fontana, A. (2000). Antibodies to the junctional adhesion molecule cause disruption of endothelial cells and do not prevent leukocyte influx into the meninges after viral or bacterial infection. J. Infect. Dis. *182*, 978–982.

Ley, K., and Kansas, G.S. (2004). Selectins in T-cell recruitment to non-lymphoid tissues and sites of inflammation. Nat. Rev. Immunol. *4*, 325–336.

Ley, K., Bullard, D.C., Arbonés, M.L., Bosse, R., Vestweber, D., Tedder, T.F., and Beaudet, A.L. (1995). Sequential contribution of L- and P-selectin to leukocyte rolling in vivo. J. Exp. Med. *181*, 669–675.

Miyasaka, M., and Tanaka, T. (2004). Lymphocyte trafficking across high endothelial venules: dogmas and enigmas. Nat. Rev. Immunol. *4*, 360–370.

Muller, W.A. (2003). Leukocyte-endothelial-cell interactions in leukocyte transmigration and the inflammatory response. Trends Immunol. *24*, 327–334.

Muller, W.A., Weigl, S.A., Deng, X., and Phillips, D.M. (1993). PECAM-1 is required for transendothelial migration of leukocytes. J. Exp. Med. *178*, 449–460.

Nathan, C. (2002). Points of control in inflammation. Nature *420*, 846–852.

Ostermann, G., Weber, K.S., Zernecke, A., Schroder, A., and Weber, C. (2002). JAM-1 is a ligand of the beta(2) integrin LFA-1 involved in transendothelial migration of leukocytes. Nat. Immunol. *3*, 151–158.

O'Sullivan, J., O'Sullivan, M., Tipton, K.F., Unzeta, M., Del Mar Hernandez, M., and Davey, G.P. (2003). The inhibition of semicarbazide-sensitive amine oxidase by aminohexoses. Biochim. Biophys. Acta *1647*, 367–371.

Portnoy, D.A., Moseley, S.L., and Falkow, S. (1981). Characterization of plasmids and plasmid-associated determinants of Yersinia enterocolitica pathogenesis. Infect. Immun. *31*, 775–782.

Pribila, J.T., Quale, A.C., Mueller, K.L., and Shimizu, Y. (2004). Integrins and T cell-mediated immunity. Annu. Rev. Immunol. *22*, 157–180.

Puri, K.D., and Springer, T.A. (1996). A schiff base with mildly oxidized carbohydrate ligands stabilizes L- selectin and not P-selectin or E-selectin rolling adhesions in shear flow. J. Biol. Chem. *271*, 5404–5413.

Rosen, S.D. (2004). Ligands for L-selectin: homing, inflammation, and beyond. Annu. Rev. Immunol. *22*, 129–156.

Salmi, M., and Jalkanen, S. (1992). A 90-kilodalton endothelial cell molecule mediating lymphocyte binding in humans. Science *257*, 1407–1409.

Salmi, M., Tohka, S., Berg, E.L., Butcher, E.C., and Jalkanen, S. (1997). Vascular adhesion protein 1 (VAP-1) mediates lymphocyte subtype-specific, selectin-independent recognition of vascular endothelium in human lymph nodes. J. Exp. Med. *186*, 589–600.

Salmi, M., Yegutkin, G., Lehvonen, R., Koskinen, K., Salminen, T., and Jalkanen, S. (2001). A cell surface amine oxidase directly controls lymphocyte migration. Immunity *14*, 265–276.

Schenkel, A.R., Mamdouh, Z., Chen, X., Liebman, R., and Muller, W.A. (2002). CD99 plays a major role in the migration of monocytes through endothelial junctions. Nat. Immunol. *3*, 143–150.

Schenkel, A.R., Mamdouh, Z., and Muller, W.A. (2004). Locomotion of monocytes on endothelium is a critical step during extravasation. Nat. Immunol. *5*, 393–400.

Smith, D.J., Salmi, M., Bono, P., Hellman, J., Leu, T., and Jalkanen, S. (1998). Cloning of vascular adhesion protein-1 reveals a novel multifunctional adhesion molecule. J. Exp. Med. *188*, 17–27.

Thompson, R.D., Noble, K.E., Larbi, K.Y., Dewar, A., Duncan, G.S., Mak, T.W., and Nourshargh, S. (2001). Platelet-endothelial cell adhesion molecule-1 (PECAM-1)-deficient mice demonstrate a transient and cytokine-specific role for PECAM-1 in leukocyte migration through the perivascular basement membrane. Blood *97*, 1854–1860.

von Andrian, U.H., and Mackay, C.R. (2000). T-cell function and migration. Two sides of the same coin. N. Engl. J. Med. *343*, 1020–1034.

von Andrian, U.H., and Mempel, T.R. (2003). Homing and cellular traffic in lymph nodes. Nat. Rev. Immunol. *3*, 867–878.

von Andrian, U.H., Hansell, P., Chambers, J.D., Berger, E.M., Torres Filho, I., Butcher, E.C., and Arfors, K.-E. (1992). L-selectin function is required for β2-integrin-mediated neutrophil adhesion at physiological shear rates in vivo. Am. J. Physiol. *263*, H1034–H1044.

Yu, P.H., Wright, S., Fan, E.H., Lun, Z.R., and Gubisne-Harberle, D. (2003). Physiological and pathological implications of semicarbazide-sensitive amine oxidase. Biochim. Biophys. Acta *1647*, 193–199.

Zhang, X., and McIntire, W.S. (1996). Cloning and sequencing of a copper-containing, topa quinone-containing monoamine oxidase from human placenta. Gene *179*, 279–286.